View metadata, citation and similar papers at core.ac.uk
brought to you by CORE
provided by UCL Discovery

A mechanism stimulating sound production from air bubbles released from a nozzle

Grant B. Deane and Helen Czerski
Scripps Institution of Oceanography, University of California San Diego, La Jolla, California 92093-0238; gdeane@ucsd.edu, hczerski@ucsd.edu

Abstract: Gas bubbles in water act as oscillators with a natural frequency inversely proportional to their radius and a quality factor determined by thermal, radiation, and viscous losses. The linear dynamics of spherical bubbles are well understood, but the excitation mechanism leading to sound production at the moment of bubble creation has been the subject of speculation. Experiments and models presented here show that sound from bubbles released from a nozzle can be excited by the rapid decrease in volume accompanying the collapse of the neck of gas which joins the bubble to its parent.

© 2008 Acoustical Society of America
PACS numbers: 43.30.Lz, 43.30.Nb [DKW]
Date Received: January 10, 2008 **Date Accepted:** February 25, 2008

1. Introduction

It has long been known that the sounds of running water are associated with the creation of bubbles.[1] The sound produced by newly formed oceanic bubbles is of interest because these bubbles enhance the flux of greenhouse gases across the ocean surface, create aerosols, and generate underwater ambient noise.[2–5] Newly formed bubbles behave like lightly damped natural oscillators responding to nonequilibrium initial conditions, and produce a short acoustic pulse at the moment of their formation.[6] Because of their importance to a wide range of subject areas, the behavior of spherical gas and cavitation bubbles has been well studied. The acoustic behavior of spherical bubbles is governed by the Rayleigh–Plesset equation, the validity of which has been verified by numerous theoretical and laboratory studies.[6–9]

2. Bubble sound excitation mechanism

There is an extensive body of literature on the acoustical properties of gas bubbles, but comparatively little is known about the mechanism driving the production of sound when bubbles are first formed. Various mechanisms have been proposed, including the increase in the internal pressure of the bubble associated with the Laplace pressure, hydrostatic pressure effects, shape mode coupling, and a fluid jet associated with the collapsing bubble neck.[9–13] Estimates of the Laplace and hydrostatic pressure effects show that they represent a minor ($<10\%$) contribution to the noise.[9] Shape mode coupling seems to play a significant role in the damping of highly distorted bubbles[14] (e.g., bubbles fragmenting in turbulence or detaching from a nozzle), but a secondary role in bubble acoustic excitation.[15]

The idea that bubble sound production is driven by the jet of water associated with the collapse of the neck of air formed immediately after bubble pinch-off was suggested by Longuet-Higgins,[16] and has been examined by Manasseh and co-workers[12,13] for rapidly (>10 Hz) sparged bubbles. Manasseh *et al.* studied the acoustic emissions of bubbles released from a nozzle with simultaneous high-speed photographs,[12] and found that the initial fall in pressure in the fluid surrounding the bubble is associated with the neck-breaking process and the rapid retraction of the tip of the bubble once it has detached. Here we will show through experiments and an analytical model that acoustic excitation can be explained by the decrease in bubble volume that accompanies neck collapse, and is driven by surface tension forces.

Bubble detachment and concurrent acoustic emission are illustrated in Fig. 1 (see Sec. 6). The pressure pulse radiated by the bubble [Fig. 1(a)] shows that the acoustic excitation begins just before detachment, and is largely complete within a single oscillation. Image I

 © 2008 Acoustical Society of America

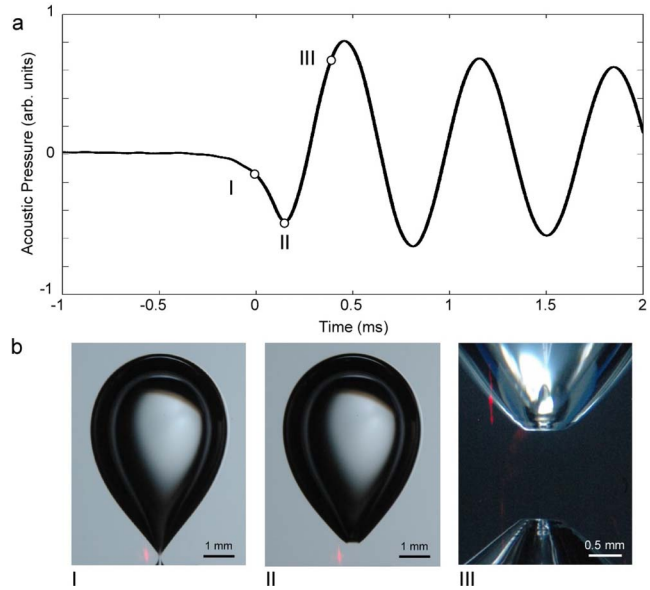

Fig. 1. (Color online) Acoustic emission and bubble release. (a) The acoustic pressure trace of a bubble released from a nozzle in the laboratory. The pressure preceding bubble release and the first few oscillations are shown. The acoustic pressure is in arbitrary units because it was measured in a small, reverberant chamber (see Sec. 6). (b) Single strobe images showing the bubble shape during acoustic excitation. The red, vertical line to the left of the bubble neck is light from the laser trigger. The release nozzle is positioned below the bottom of the images. The time of the images relative to the pressure trace is indicated by roman numerals. Image I shows the bubble immediately prior to neck rupture. Image II shows the state of neck collapse at the first pressure minimum. Image III shows a magnified view of the collapsing neck. A small, reentrant jet can be seen forming at the base of the neck and capillary waves can be seen propagating along the neck.

shows the bubble shape immediately prior to detachment. Image II, taken 160 μs after detachment, illustrates the rapid collapse of the neck remnant. Image III, taken 320 μs after detachment, shows a small reentrant jet of water forming within the collapsing neck.

3. Model for neck collapse

A simple analytical model of neck collapse can be developed as follows. Immediately preceding rupture, the bubble geometry is divided into a sphere, a cone, and a hyperbolic region (Fig. 2). The behavior of the hyperbolic region up to the point of neck rupture has been studied.[16,17] Our calculations show that it represents only a small fraction of the total volume of the collapsing neck and plays a minor role in bubble acoustic excitation. Accordingly, it is modeled as a simple cylinder of length x_0 and radius r_0. The conical region is characterized by its slope, η. For the bubble illustrated in Fig. 1, $\eta \approx 0.84$.

The radius of curvature at the neck end during collapse is small, resulting in a large Laplace pressure jump across the boundary and rapid inward acceleration. We begin by assuming that the surface tension energy in a frustrum of neck is converted into kinetic energy of the fluid within it. Following this line of reasoning yields expressions for the neck velocity in terms of distance along the neck measured from the point of rupture, x:

$$u = \begin{cases} \left(\dfrac{4\sigma}{\rho r_0}\right)^{1/2}, & x < x_0 \\ \left(\dfrac{4\sigma(1+\eta^2)^{1/2}}{\rho \eta x}\right)^{1/2}, & x \geq x_0, \end{cases} \tag{1}$$

where σ is the fluid surface tension and ρ is the fluid density. The neck collapse time is found by integrating the reciprocal of the velocity over x:

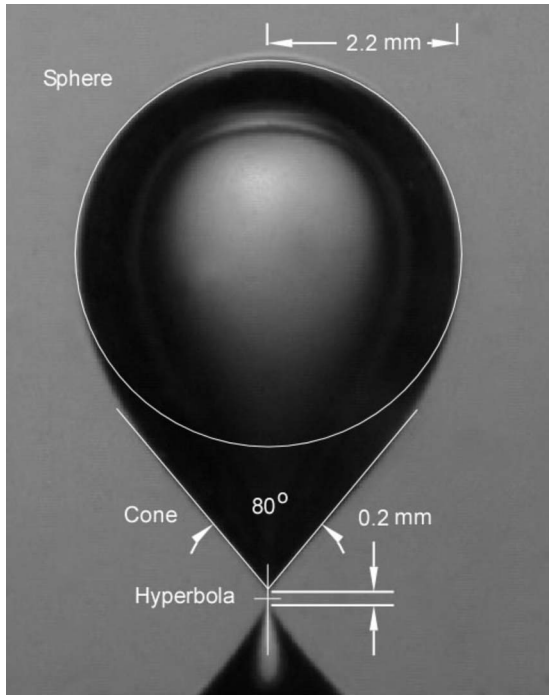

Fig. 2. Geometry for the neck collapse model.

$$\tau = \begin{cases} \left(\dfrac{\rho r_0}{4\sigma}\right)^{1/2} x, & x < x_0 \\ \left(\dfrac{\rho r_0}{4\sigma}\right)^{1/2} x_0 + \dfrac{2}{3\eta}\left(\dfrac{\rho}{4\sigma(1+\eta^2)^{1/2}}\right)^{1/2}\left[(r_0+\eta(x-x_0))^{3/2} - r_0^{3/2}\right], & x \geq x_0. \end{cases} \tag{2}$$

The velocity and collapse time are plotted in Fig. 3 as a function of x along with measurements of these quantities for the bubble illustrated in Fig. 2 (see Sec. 6). Neglecting the small volume of the hyperbolic region by setting $x_0 = r_0 = 0$, Eq. (2) can be used to calculate the decrease in neck volume with time:

$$\Delta V = -\frac{3\pi\sigma\eta(1+\eta^2)^{1/2}}{\rho} t^2. \tag{3}$$

where $t = 0$ at the moment of neck rupture.

4. Forcing term in the Rayleigh–Plesset equation

The rapidly changing neck volume drives the bubble into breathing mode oscillations. The dynamics of the collapse are inherently nonspherical, but we assume that the breathing mode response of the bubble can be described assuming spherical symmetry. To drive the bubble, we have calculated the change in external pressure that would be required to account for the change in bubble volume associated with the neck collapse. The decreasing volume results in an increase in pressure inside the bubble, which can be calculated by assuming the polytropic relationship:

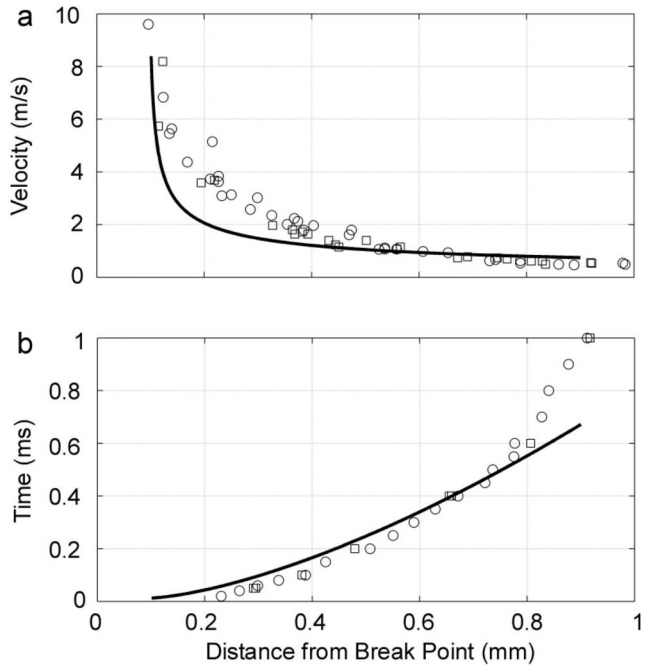

Fig. 3. Comparison of neck collapse model with experimental data. Circles and squares respectively correspond to fresh and salt water measurements for r_0=4.5 μm and x_0=100 μm. The cylinder radius was determined from the neck velocity at the end of cylinder collapse and the cylinder length was estimated from the bubble photographs. (a) The velocity of the base of the collapsing neck as a function of distance from the rupture point. (b) The collapse time versus distance from the rupture point.

$$p_{\text{in}} = p_{\text{in},0}\left(\frac{V_0}{V_0 + \Delta V}\right)^{\kappa}, \tag{4}$$

where p_{in} is the gas pressure internal to the bubble, $p_{\text{in},0}$ is the equilibrium pressure inside the bubble, V_0 is the equilibrium volume of the bubble, κ is the gas polytropic index, and we have neglected thermal losses associated with gas compression driven by the neck collapse. Thermal losses due to the natural response of the bubble are accounted for using an effective thermal viscosity, μ_{th}, as described by Prosperetti.[7] The required external pressure change is calculated from Eq. (4) by invoking continuity of normal stress across the bubble wall and neglecting surface tension and viscous forces there. The final result is a driving term on the right hand side of the linearized Rayleigh–Plesset equation:

$$\frac{\partial^2 \varepsilon}{\partial t^2} + \left[\frac{4(\mu + \mu_{\text{th}})}{\rho R_0^2} + \frac{kR_0}{1 + k^2 R_0^2}\omega\right]\frac{\partial \varepsilon}{\partial t} + \left[\frac{3\kappa p_{in,0}}{\rho R_0^2} - \frac{2\sigma}{\rho R_0^3} + \frac{k^2 R_0^2}{1 + k^2 R_0^2}\omega^2\right]\varepsilon = f(t), \tag{5}$$

where ε is the fractional increase in bubble radius, μ is the fluid viscosity, k and ω, respectively, are the wave number and angular frequency of sound at bubble resonance, R_0 is the bubble equilibrium radius, and the forcing function is given by

$$f(t) = -\frac{9\kappa\sigma\eta p_{in,0}(1 + \eta^2)^{1/2}}{4\rho^2 R_0^5} t^2; \quad t > 0. \tag{6}$$

In deriving Eq. (5), we have assumed that the velocity and displacement coefficients inside the square brackets are constant and take the values they have at the bubble's natural frequency. For the approximately 2 mm bubbles we are studying, the frequency-dependent radiation term (the k term in square brackets multiplying ε) is less than 1/5000 of the dominant pressure term and

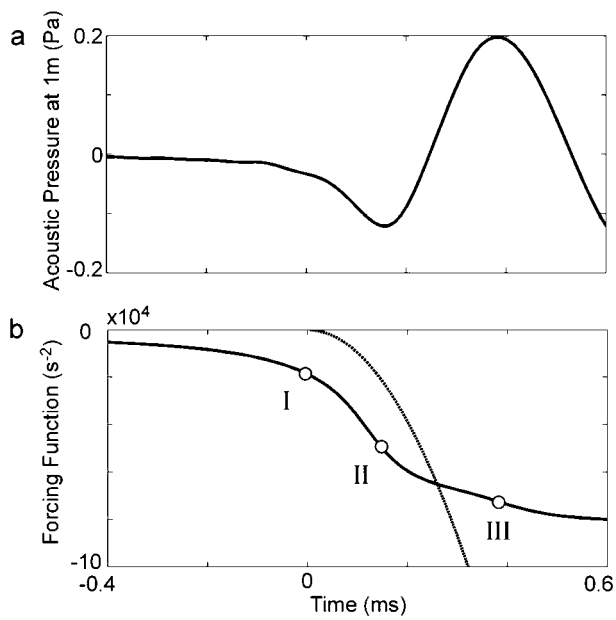

Fig. 4. Comparison of forcing function calculations with experimental data. (a) The acoustic pressure trace from a bubble released in a large pool. The bubble size and release nozzle were similar to those for the photographed bubbles. (b) The measured and theoretical forcing functions. The solid line is the measured forcing function, determined from analysis of bubble emissions. The roman numerals indicate the time of the images shown in Fig. 1. The dotted line corresponds to the forcing function calculated according to Eq. (6) with R_0=2.2 mm, σ =0.072 N/m, ρ=1000 kg/m^3, κ=1.4, and η=0.84.

can be neglected. The frequency-dependent effects of damping have been estimated (see below), and can also be ignored.

The initial shape of the radiated acoustic pulse can be analyzed to provide an estimate of the bubble forcing function, which can then be compared with Eq. (6). Although we measured the bubble acoustic signature in a small, acrylic chamber, we have not analyzed it because of the effects of reverberation. The problem with reverberation is not the level of signal which it contributes to the hydrophone output, but rather that it represents a coherent driving signal with a specific phase on the bubble wall.[18] To mitigate this problem, we have analyzed acoustic pulses recorded in a reverberation-limited test pool[19] radiated by bubbles of the same size (within 10%) and released from the same nozzle as those photographed in the small acrylic chamber but at a depth of 2 m (within 5%). These measurements were made with an International Transducer Corporation 6050C hydrophone. Because the nearest reflecting boundary is 2 m distant, the first 2.7 ms of the bubble signature is free from the effects of reverberation.

The acceleration of the bubble wall can be calculated from the acoustic radiation using $\partial^2\varepsilon/\partial t^2 = p_a/(\rho R_0^3)$, where p_a is the acoustic pressure 1 m from the bubble.[6] Note that an initial inward acceleration of the bubble wall results in the radiation of a rarefaction. The acceleration can then be integrated once to obtain $\partial\varepsilon/\partial t$ and again to obtain ε. The first three terms in Eq. (5) are then summed to obtain $f(t)$. This procedure is similar to that carried out by Pumphrey and Elmore,[20] who computed the bubble wall motion from analytical expressions for the acoustic field. Here we apply this technique to the measured field, which enables us to compute the driving term on the Rayleigh–Plesset equation. The result of the procedure is shown in Fig. 4. The top trace shows the reverberation-limited acoustic field. The bottom trace shows the mean forcing function estimated from 84 bubbles compared with Eq. (6). Approximately 1/4 of the forcing occurs before the neck detachment, presumably driven by the radial influx of the neck walls before rupture, but the main part of the excitation occurs during neck collapse. The forc-

ing function was calculated with no damping and with ten times measured damping to explore its effects (not shown). The case of no damping produced essentially no change in the forcing function, while ten times damping changed the forcing function estimate by less than 10%.

The general shape and magnitude of the forcing is adequately accounted for by the neck collapse theory once predetachment forcing is allowed for. The neck collapse model does not contain any dissipation mechanisms and does not model the collapse behavior past the first few hundred microseconds, so the theoretical curve deviates significantly from the measured response for times greater than a few hundred microseconds.

5. Concluding remarks

We have shown that the sound produced by a bubble released from a nozzle can be explained by the collapse of the neck of air formed immediately after bubble pinch-off. The collapsing neck decreases the bubble volume and excites the bubble into oscillation. The initial response of the bubble depends on the time scale of the neck collapse and the natural frequency of the bubble. This can be seen in the width of the first rarefaction trough of the acoustic pressure trace in Fig. 1, which is noticeably less than subsequent troughs. No significant differences were observed in the neck collapse process between fresh and salt water. The collapse is driven by surface tension energy in the neck, and a simple energy balance model gives a first-order description of the process. The change in bubble volume associated with the neck collapse can be incorporated into the linearized Rayleigh–Plesset equation to derive an acoustic forcing function. An estimate of this function based on the analysis of bubble acoustic emissions compares favorably with the model predictions.

We believe that the role of neck collapse in stimulating bubble sound is not limited to nozzle release. Surface tension energy has been implicated in the acoustic stimulation of fragmenting bubbles,[15,19] and it is probable that neck collapse drives sound production from fragmentation and therefore noise production by breaking waves.[21]

6. Methods summary

The bubble-release nozzle was positioned 5 cm above the base of a transparent acrylic tank with a 13-cm-square cross section. The tank was filled with either fresh or salt water to a depth of 25 cm. An International Transducer Corporation 1089D was placed alongside the nozzle tip, approximately 1 cm from the bubble. Air bubbles were released at a nominal rate of ten per minute. Bubble release was determined by interruption of a laser beam directed through the neck region, which was used to trigger data acquisition and flash lighting. Flashes from two strobe lights, each of 15 μs duration, illuminated the bubble with a preprogrammed interval. Both images were superposed on a single frame, permitting observation of the neck development over short time intervals relative to the moment of neck rupture. The neck displacements were measured by increasing the inter-flash interval, with the first flash simultaneous with neck rupture. The neck velocity was measured using a short inter-flash interval with flash pairs occurring at successively later times after neck rupture. The reverberation-limited bubble signature measurements were taken during the experiment described in Deane and Stokes.[19]

Acknowledgments

We thank Dr. Dale Stokes and Cary Humphries for assistance with the acoustic data collection, and Dr. David Farmer for discussions. We acknowledge financial support from the National Science Foundation and the Office of Naval Research. We are also grateful to two anonymous reviewers who helped us improve the manuscript.

References and links

[1]M. Minnaert, "On musical air bubbles and the sounds of running water," Philos. Mag. **16**, 235–248 (1933).
[2]E. Lamarre and W. K. Melville, "Air entrainment and dissipation in breaking waves," Nature (London) **351**, 469–472 (1991).
[3]C. D. O'Dowd and G. de Leeuw, "Marine aerosol production: A review of the current knowledge," Philos. Trans. R. Soc. London, Ser. A **365**, 1753–1774 (2007).
[4]D. M. Farmer, C. L. McNeil, and B. D. Johnson, "Evidence for the importance of bubbles in increasing air-sea

gas flux," Nature (London) **361**, 620–623 (1993).
[5]W. K. Melville, "The role of surface-wave breaking in air-sea interaction," Annu. Rev. Fluid Mech. **28**, 279–321 (1996).
[6]T. G. Leighton, *The Acoustic Bubble* (Academic, London, 1994).
[7]A. Prosperetti, "Thermal effects and damping mechanisms in the forced radial oscillations of gas bubbles in liquids," J. Acoust. Soc. Am. **61**, 17–27 (1977).
[8]M. S. Plesset and A. Prosperetti, "Bubble dynamics and cavitation," Annu. Rev. Fluid Mech. **9**, 145–185 (1977).
[9]H. C. Pumphrey and J. E. Ffowcs Williams, "Bubbles as sources of ambient noise," IEEE J. Ocean. Eng. **15**, 268–274 (1990).
[10]M. S. Longuet-Higgins, "An analytic model of sound produced by raindrops," J. Fluid Mech. **214**, 395–410 (1990).
[11]R. D. Hollet and R. M. Heitmeyer, "Noise generation by bubbles formed in breaking waves," *Sea Surface Sound* (Kluwer, Boston, 1998).
[12]R. Manasseh, S. Yoshida, and M. Rudman, "Bubble formation processes and bubble acoustic signals," *Proceedings of the Third International Conference on Multiphase Flow (ICMF'98)*, Lyon, France, 8–12 June 1998, paper no. 202 (CD-ROM).
[13]R. Manasseh, A. Bui, J. Sandercock, and A. Ooi, "Sound emission processes on bubble detachment," *Proceedings of the 14th Australasian Fluid Mechanics Conference*, Adelaide, South Australia, edited by B. B. Dally, 9–14 December 2001, Vol. **1**, pp. 857–860.
[14]M. S. Longuet-Higgins, "Nonlinear damping of bubble oscillations by resonant interaction," J. Acoust. Soc. Am. **91**, 1414–1422 (1992).
[15]G. B. Deane and M. D. Stokes, "The acoustic emissions and energetic of fragmenting bubbles," J. Acoust. Soc. Am. (in review).
[16]M. S. Longuet-Higgins, "The release of air bubbles form an underwater nozzle," J. Fluid Mech. **230**, 365–390 (1991).
[17]S. T. Thoroddsen, T. G. Etoh, and K. Takehara, "Experiments on bubble pinch-off," Phys. Fluids **19**, 042101 (2007).
[18]T. G. Leighton, P. R. White, C. L. Morfey, J. W. L Clarke, G. J. Heald, H. A. Dumbrell, and K. R. Holland, "The effect of reverberation on the damping of bubbles," J. Acoust. Soc. Am. **112**, 1366–1376 (2002).
[19]G. B. Deane and M. D. Stokes, "The acoustic signature of bubbles fragmenting in sheared flow," J. Acoust. Soc. Am. **120**, EL84–EL89 (2006).
[20]H. C. Pumphrey and P. A. Elmore, "The entrainment of bubbles by drop impacts," J. Fluid Mech. **220**, 539–567 (1990).
[21]G. B. Deane and M. D. Stokes, "Scale dependence of bubble creation mechanisms in breaking waves," Nature (London) **418**, 839–844 (2002).